Evaluation of the surface chemistry and drug-polymer interaction of semi-crystalline micro-particles for the development of controlled release formulations

Article (Accepted Version)

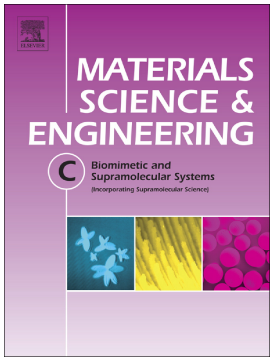

Evaluation of the surface chemistry and drug-polymer interaction of semi-crystalline micro-particles for the development of controlled release formulations

Sadeque H. Mithu, Syed N. Haque, Babur Z. Chowdhry, Ali Nokhodchi, Mohammed Maniruzzaman

PII: S0928-4931(16)32253-6
DOI: doi: 10.1016/j.msec.2017.03.154
Reference: MSC 7666

To appear in: *Materials Science & Engineering C*

Received date: 18 November 2016
Revised date: 12 March 2017
Accepted date: 14 March 2017

Please cite this article as: Sadeque H. Mithu, Syed N. Haque, Babur Z. Chowdhry, Ali Nokhodchi, Mohammed Maniruzzaman , Evaluation of the surface chemistry and drug-polymer interaction of semi-crystalline micro-particles for the development of controlled release formulations. The address for the corresponding author was captured as affiliation for all authors. Please check if appropriate. Msc(2017), doi: 10.1016/j.msec.2017.03.154

Evaluation of the surface chemistry and drug-polymer interaction of semi-crystalline micro-particles for the development of controlled release formulations

Sadeque H. Mithu[1], Syed N. Haque[1], Babur Z. Chowdhry[1], Ali Nokhodchi[2, 3], Mohammed Maniruzzaman[2*]

[1]Faculty of Engineering and Sciences, University of Greenwich, Chatham Maritime, Chatham, Kent ME4 4TB; [2]Department of Pharmacy, School of Life Sciences, University of Sussex, Falmer, Brighton, BN1 9QT; [3]Drug Applied Research Center and Faculty of Pharmacy, Tabriz University of Medical Sciences, Tabriz, Iran.

Correspondence: M Maniruzzaman (M.Maniruzzaman@sussex.ac.uk or M.Maniruzzaman12@gmail.com), A Nokhodchi (A.Nokhodchi@sussex.ac.uk)

ABSTRACT

This research work explores the surface chemistry and drug-polymer interaction in the manufactured controlled release micro-particles. Isoniazid (INH) was used as a model anti-tubercular drug while Eudragit® S100 (S100), Eudragit®L100-55 based co-processed Acryl EZE (EZE) and Ethylcellulose ECN10 (ECN10) were used as polymeric carriers. INH containing micro-particles were prepared using a mini spray dryer B-290 (Buchi, Switzerland). The drug polymer ratios were optimized at 1:1 and 1:3 to evaluate the effect of polymers on the release of the drug from the micro-particles. Solid state characterization via SEM and particle size analysis of the manufactured micro-particles showed densely aggregated spherical particles with a mean diameter less than 10 µm. The advanced surface analysis via EDS revealed a homogenous drug distribution on the spray dried micro-particles. The physico-chemical characterization carried out by using DSC and XRPD showed an increase in the amorphicity of the drug during the spray drying process while the chemical elemental analysis via XPS revealed a strong intermolecular interaction between the amine group of the drug and the carboxyl group of the polymers. As expected, the *in vitro* dissolution study showed a slow release pattern for the highly water soluble drug INH in acidic media (pH 1.2) for the first 2 h followed by a burst release upon changing the pH to 6.8. It was concluded that emerging spray drying processing can be used as a valuable tool to encapsulate drug for controlled release dosage forms by means of facilitating a possible drug/polymer interaction as outlined by novel XPS analysis.

Keywords: Microencapsulation, spray drying, controlled release, amorphous, crystalline, micro-particles.

ABBREVIATIONS

ANOVA	Analysis of variation
BE	Binding energy
DL	Drug loading
DSC	Differential scanning calorimetry
ECN10	Ethyl Cellulose N10
EDS	Energy dispersive X-ray
EE	Encapsulation efficiency
EZE	Eudragit L100-55 (Acryl EZE)
HPLC	High performance liquid chromatography
INH	Isoniazid
S100	Eudragit S100
SEM	Scanning electron microscopy
SSA	Specific surface area
XPS	X-ray photoelectron spectroscopy
XRPD	X-ray powder diffraction

1. Introduction

'Microencapsulation' via spray drying process is referred to a technique in which a drug in the form of a solid or liquid is encapsulated in a biocompatible and/or biodegradable polymeric matrix or pharmaceutically acceptable excipients [1]. Generally, by means of this process, the produced particles are with a diameter in the range of 1 to 1000 micrometers [1]. Microencapsulation technique has various pharmaceutical applications such as preparation of sustained or prolonged release medications, single layer tablet containing chemically incompatible ingredients and new formulation concepts for creams, aerosols, plasters, surgical dressings, injectable [2-5]. In the case of drugs that are poorly water soluble, microencapsulation process is carried out to achieve its increased dissolution rate with a fast onset of action [1, 5]. In recent years, microencapsulation process using spray drying technique has become quite popular due to its industrial adaptability and ease of scale up process meeting the regulatory requirements [1-5].

Spray drying is, in general term, the transformation of feed (solution, suspension or emulsion) from a fluid state into a dried particulate form by means of spraying the feeding solutions into a hot drying medium (cyclone). Spray drying is a unique process whereby the final product complies with the standards concerning particle size, particle size distribution, particle shape, moisture content and bulk density in a single step operation [1, 3, 5, 6-10]. Due to rapid solvent evaporation, spray drying is widely used in the drying of foodstuffs, pharmaceuticals, ceramics and many other substances. The most important aspect of spray drying is the automization of suspension into hot drying medium (usually air). The formation

of a fine spray due to automization is the most important factor to gain economic production of top quality products, by maintaining optimum conditions for evaporation [1, 6-12].

Controlled release drug delivery systems are aimed at achieving more predictable bioavailability of drugs and help in optimizing pharmaco-therapies. As compared to conventional dosage forms, these systems provide improved efficacy, reduced side effects and avoid issue with the patient compliances [2-4]. Out of all dosage forms such as tablets or capsules, microparticles have significant advantages such as protection of drug from the gastrointestinal tract by administrating through intramuscular or subcutaneous route, ease of administration, target specific drug delivery and no need for surgery to remove empty remnants [1, 2, 5].

Polymers can be used for the purpose of prolonging the release and in turn bioavailability by encapsulating the active ingredient in the polymeric matrix or shell. Various polymers such as Eudragit polymers, cellulose derivatives and some natural polymers have been successfully used in the preparation of delivery systems by spray drying. The success of the process depends on a number of factors such as the type of feed, the degree of core material encapsulation and the drug/polymer ratio [13, 14].

Isoniazid (INH) is a first line antitubercular drug used for the prophylaxis and therapy of tuberculosis caused by *mycobacterium tuberculosis*. The most probable mechanism of action of isoniazid is the inhibition of synthesis of mycolic acids which is a unique component of mycobacterium cell wall [15, 16]. Due to its pharmacokinetics and pharmacological properties, controlled release dosage forms of INH are prepared so that it would maximize therapeutic efficacy, reduce dosing intervals and dose related adverse effects [16]. INH is soluble in water (~14% at 25ºC, ~26% at 40ºC), with a pKa value of about 1.82 and Log P 0.64, LD_{50} 100 mg/kg (Human, oral) [16, 17].

The aim of this study was to optimize and prepare INH loaded microparticles by means of spray drying techniques. For the first time, an EDS and XPS were combined to study the surface chemistry of the spray dried particles. The novelty of this reported study lies on the exploitation of novel EDS and XPS techniques to analyse the surface of the manufactured micro-particles and outline chemical interactions between the drug and polymers, respectively. Organic dispersions of either Eudragit S100 and Acryl EZE or ethyl cellulose derivatives with various drug/polymer ratios were evaluated to develop controlled release drug delivery systems of INH.

2. Materials and Method

2.1 Materials

Isoniazid (INH) was purchased from Sigma Aldrich (Gillingham, UK). The polymers Ethyl Cellulose N10 (ECN10) was kindly donated by Harkeulus (Germany). Eudragit S100 (S100) and Eudragit L100-55 based co-processed polymer Acryl-EZE (EZE) was kindly provided by Evonik Industries (Germany) and Colorcon Ltd (Dartford, UK), respectively. Absolute ethanol and other solvents for HPLC were of laboratory/pharmaceutical grade and obtained from Fisher scientific (UK).

2.2 Spray drying process

The microencapsulation process was performed in a B-290 mini spray dryer (Buchi, Basel, Switzerland). Various drug/polymer binary mixtures (1:1 and 1:3) were dissolved in ethanol (100 mL) as shown in Table 1. The processing parameters for all spray drying processes are also summarized in Table 1. Briefly, the inlet temperature was set at 100^{o}C while the outlet at 60^{o}C, the aspirator at 90% with a feed solution rate of 13-15%. The encapsulation yield was also calculated as the ratio of the mass of the microencapsulated

particles obtained during the process to the mass of the initial substances added (drug and polymer)

Bulk and tap densities of the spray dried powder were also measured by taking about 1 g of sample and placing it in a 10 mL measuring cylinder. The initial reading was taken as volume. The powder in the cylinder was tapped 100 times onto a rubber mat with the help of a Tap Machine. This process was repeated 3 times. The final reading of the cylinder was then recorded and the tap density was calculated.

The entrapment efficiency and drug loading of INH in various formulations were determined according to the following procedure: approximately 20 mg of the spray dried INH loaded microparticles was weighted and dispersed into 10 mL of phosphate buffer solution (pH 7.2). The mixture was continuously stirred with magnetic stirrer for 24 h followed by a sonication at room temperature for 30 min. The solution was then centrifuged at 7000 rpm for 15 min (Sorval RC6 Plus) and the supernatant was collected via the filtration of the solutions using 45 μm pore membrane. The amount of drug encapsulated was determined by determining by HPLC as per the method described below in section 2.9. The entrapment efficiency and the drug loading was evaluated via using the following equations (Eqs. 1 and 2):

$$Drug\ \ Loading\ (\%) = \frac{Calculated\ \ Mass\ of\ \ Drug}{Mass\ of\ \ Drug\ Loaded\ Microparticles}\ \mathrm{X}\quad 100 \qquad (1)$$

$$Encapsulation\ Efficiency\ \ (\%) = \frac{Actual\ \ Drug\ Loading}{Theoritical\ Drug\ Loading}\ \mathrm{X}\quad 100 \qquad (2)$$

2.3 Particle size analysis

The particle size distributions of all spray dried powders were determined using a Mastersizer 2000 laser diffraction instrument (Malvern Instruments, UK) with a dry powder

sample dispersion accessory (Scirocco 2000). The pressure was set at 2 bars and a vibration feed rate of 50%. All samples were run in triplicate. Mastersizer 2000 software was used for all data evaluation and interpretations as well as to calculate the d(50) which is the geometric median particle size and the d(10) and d(90) which are the particle diameters at 10% and 90% of the cumulative volume distribution, respectively. The span referred to the width of the distribution relative to the d(50) was calculated using the following equation (Eq. 3).

$$Span = \frac{[d_{(90)} - d_{(10)}]}{d_{(50)}} \qquad (3)$$

2.4 Scanning Electron Microscopy (SEM)/ EDS analysis

Micrographs of pure drugs and spray dried powders were obtained by a scanning electron microscopy using a JEOL JSM-5310LV machine (JEOL, Tokyo, Japan) at 15kV accelerating voltage, 20 mm working distance, spot size 14, secondary electron detector. Elemental assays and mapping were also undertaken using an AZtec Energy Dispersive X-ray microanalysis system with 50 mm^2 X-Max detector (EDS) (Oxford Instruments, UK). For the purpose of the analysis, all samples were placed on double sided adhesive carbon tapes stuck on aluminium stubs. All samples were then coated with a thin layer of carbon by using an Edwards 306 high vacuum carbon evaporator prior to each analysis.

2.5 X-Ray Powder Diffraction (XRPD)

For XRPD studies a Bruker D-8 Advance (Germany) system was used. The experiment was carried out at an angle of 2-40 2-theta values. The sample was rotated at 15 rpm and the exit slit used was 0.2 mm. The opening angle was 3^0. The generator condition was set at 40 kv and 40 mA. The counting time was 0.1 seconds per step. Lynex Eye controller was used.

2.6 Differential Scanning colorimetry

The solid state of the pure drug, polymers and the spray dried powders was studied using a differential scanning colorimetry (DSC) G823e machine (Mettler Toledo, USA). Approximately, 1-2 mg of each sample were loaded in aluminum crucibles and sealed under crucible press and then the lid was pierced. The crucibles were placed in DSC and the samples were heated from 25^{o}C to 250^{o}C with a heating rate of 10^{o}C/min under nitrogen. STARe thermal analysis software was used for data analysis.

2.7 X-ray photoelectron spectroscopy (XPS)

The XPS was performed to analyze the first layer atomic structure of the formulations via a Kratos Axis Ultra-DLD using a monochromatic Al K_{α} X-ray source (120 W) and an analyzer pass energy of 160 eV (survey scans) or 20 eV (high resolution scans). The operating pressure during analysis was optimized at 1×10^{-9} Torr. The C (1s) signal at 285.0 eV was used as a reference signal for all data and was attributable to unsaturated C-C/C-H bonds. CasaXPS^{TM} (Version 2.3.15) software was used for the quantification and curve fitting of all formulations run in the XPS analysis.

2.8 Dissolution studies

The dissolution studies were performed using Varian 705 DS. The temperature of the dissolution bath was maintained at 37^{o}C and the stirring rate at 100 rpm. The dissolution medium used was 750 ml 0.1 N HCl solution of pH 1.2 for first two hours. The pH was then changed to 6.8 by using 150 ml phosphate buffer after 2 h. The spray dried samples of about 100 mg equivalent of INH was used in each vessel. About 2-3 ml samples were withdrawn at an interval of 0.5, 1, 2, 3, 5 and 12 h and filtered prior to collect them in airtight glass vials. All samples were run in triplicates (n=3).

2.9 High Performance Liquid Chromatography (HPLC)

The released INH amount was determined by using HPLC 1200 series (Aligent Technologies) and detected at 266 nm using a variable wavelength detector. The column used was HICHROM H50DS 3801 and the mobile phase methanol: water (60:40). The flow rate was maintained at 1.5 ml/min. various standard solution ranging 10-50 µm/ml were used to plot a calibration curve and calculated the drug release profile of INH.

2.10 Release mechanism

Zero order kinetics, first order kinetics, Hixson–Crowell, Higuchi and Korsmeyer–Peppas models were used for the analysis of the dissolution mechanism taking the rate constant obtained from these models as an apparent rate constant. The drug release patterns were analysed by release kinetics theories using a software suite DDSolver [18].

2.11 Statistical analysis

The samples were compared with the reference (control) by an analysis of variance (ANOVA) test. The Microsoft Excel (MS 2013, USA) software was used to perform all statistical analyses. The P-value < 0.05 was considered as significant. All the results are expressed as mean ± standard deviation.

3. Results and Discussion

3.1 Spray drying processing

Various parameters used to manufacture microencapsulated particles of isoniazid/polymers using the spray drying processing as well as the drug loading and encapsulation efficiency are summarized in Table 1. All drug and polymers used in this study were polar in nature and depicted in Figure 1. The difference in the yield was observed in the case of different polymers and formulations and some portion of the product was lost due to either the exhaust gas in the cyclone or some product being adhered to the cyclone. The highest yield was obtained in the case of ethyl cellulose derivatives (EC 10) with different

drug/polymer ratios. As can be seen in Table 1, the drug entrapment efficiency (%) varies from 81-94.4 % which are relatively high in regards with a theorical drug loading of 25% w/w (actual drug loading 22.8-23.6% w/w) and 50% w/w (actual drug loading 40.5-45.1 % w/w). Interestingly, there was not that significant diffenerce observed in the values of actual drug loading and the entrapment efficiency of the drug between various polymers (with the same ratios). The high entrapment efficiency reflects the optimized process and most importantly the drug polymer miscibility/interactions. It can also be claimed that the optimized process and the formulation compositions can be utilized to develop novel formulations without compromising the high drug entrapment/encapsulation efficiency.

Generally, it is expected that a high drying or inlet temperature will result in a faster drying rate leading to a higher productivity of the spray dried powders. Since the drying temperature used in this study was relatively high (100^{o}C) in the presence of organic solvents, the percentage yield of all formulations was satisfactorily above the average (50-60%) that typically achieved in a spray drying technique. It has been reported in the literature that the high air inlet temperature normally causes an excessive evaporation and cracks the membrane resulting in high amount of encapsulated ingredients collected [2, 19]. Similarly, the drying rate applied in this study produced the higher ratio of surface to volume for the spray-dried particles resulting in the lower density of the powders (Table 2) [20]. Calculated bulk and tap density results for all spray dried formulations are represented in Table 2. It will be interesting to investigate the effect of this low density of the particles on the controlled release of the anti-tubercular agent INH.

Particle size distributions on the basis of volume mean diameter for all spray dried formulations were narrow and monomodal with low span values. The calculated span values were between 1.1 and 1.2 for S100 systems, between 1.1 to 1.3 for EZE and between 1.0 and 1.2 for EC10 while the specific surface area (SSA) was in between 68.15-106.90 m^2/g. The

geometric median particle size (d50) of all spray dried particles was in the range of 5.7–6.0 μm while the d(10) and d(90) stayed between 1.2-1.3 μm and 8.3-9.4 μm, respectively as the spray drying process was optimised. The study of the loss on drying (LoD) revealed that a minimal amount of moisture or residue solvent was left in the micro-particles after the spray drying process. It was observed that only about ~2% (w/w) was lost in the LoD experiments making it a suitable processing technology to satisfy the use of organic solvents and regulatory requirements.

3.2 Particle morphology and surface analysis

The micrographs of INH loaded formulations revealed spherical shaped particles (Fig. 2a). No drug crystals were seen on the surface of the spray dried micro-nano particles even at relatively high magnifications (magnifications up to X 30.0 K). This simply indicates that the highly crystalline INH particles have been encapsulated/coated by the amorphous polymers and hence the spherical particles seen under the microscope represents mainly the polymer. Interestingly, it has been seen that a large number of particles fell in the nano-sized range which may prove efficient for developing some drug molecule to overcome solubility issues.

A further analysis of SEM/EDS undertaken to elucidate the presence and distribution of the drug particles in the spray dried polymeric matrices showed a homogenous distribution of the drug throughout. From the structural analysis of the drug and the polymers used as shown in Fig. 1, only the drug has nitrogen (N) atoms in its structure while both polymers are made of mainly O and C. Therefore, an elemental analysis of N atoms in all spray dried particles will indicate the homogeneity of the drug distribution. Therefore, for the purpose of this study, N atoms were used as a marker to confirm the presence of the drug in the

microencapsulated polymeric matrices. The distribution of the drug was experimented by implementing the EDS elemental mapping of N atoms (Fig. 2b). The EDS mapping showed that majority of the area was covered by the O and C which was expected as most of the organic drugs and polymers are composed of mainly these two atoms, likewise the drug and the polymers used in this study. As results of this, in all spray dried particles, the amount of N present comprised comparatively the least proportion of all of the other elements.

As depicted in Fig. 2b, the bulk INH represented a homogenous distribution of the marker atoms (N) indicated by the deep blue color in EDS mapping. Any presence of N atoms in any of the spray dried formulations would have indicated the presence of the N containing drug INH. From Fig. 2b, it is obvious that INH was homogenously distributed in the spray dried microcapsules as indicated by the blue color. The image showed that the distribution of N atoms in the INH/S100 systems is homogeneous throughout the particle captured in the microscope. The data presented from the advanced EDS analysis of INH/S100 showed complementing results compared to that of pure INH. The foregoing is supported by the literature as well [21, 22].

3.3 XRPD studies

The crystallinity of the drug in the microencapsulated particles was analyzed by X–ray diffraction. As can be seen in Fig. 3, the diffractogram of pure INH exhibited major distinct intensity peaks at various 2-theta positions ranging from 10 to 30 2θ degrees while the polymers (S100 and ECN10) exhibited peaks due to their amorphous nature. However, the co-processed Acryl EZE showed some characteristic peaks due to the presence of crystalline materials in the structure (data not shown). The spray dried micro-nano particles showed identical low intense peak due to the presence of crystalline INH in the formulations. The reduction in the intensity of the crystallinity indicated the increase in the amorphicity of the drug present in the spray dried powders. Apparently, it has been seen that the increase in

the amount of polymers in the formulations resulted in the decrease in the crystallinity for all drug/polymer compositions.

3.4 Thermal analysis

The solid state of the drug, bulk polymer and the formulations were studied by the DSC. Fig. 4a depicts the DSC traces of the pure drug and the polymers. The highly crystalline (crystallinity higher than 92%) INH showed a sharp thermal endothermic event at 172.10^{o}C due to its melting with the enthalpy, ΔH = 222.35 J/g. The thermal analysis of the bulk polymers showed that unlike S100 and ECN10, EZE exhibited a crystalline thermal transitions at about 75^{o}C which corresponds to the melting of the crystalline substances present in the co-processed polymer. Similar findings have been reported elsewhere [23]. The amorphous S100 and ECN10 showed a thermal event at about 165^{o}C and 133^{o}C, respectively corresponding to their glass transitions.

Fig. 4b shows the detailed thermal events of the spray dried formulations. The formulation containing ECN10 as carrier showed significant shifts on both the melting transition and the Tg of the polymer. This could be attributed to the possible drug/polymer interactions. Interestingly, with the increase in the polymer contents in the formulations, the melting point of the drug has been reduced significantly to 139.31 ^{o}C but the Tg has been slightly increased. This is expected as the increased amount of the polymer present in the systems have contributed to the increased Tg values. Quite similar results were observed for other polymers. The overall findings from the DSC traces can claim that the shifts of the INH melting points may have been attributed to the amorphicity increase of the drug as complemented by XRPD data or this could also happen due to the solublisation of the drug in the polymeric matrices used during the spray drying. The traces corresponding to the melting of the drug in the spray dried system were visible at 133.30-164.12^{o}C depending on the Tg and nature of the polymers.

3.5 Surface elemental analysis via XPS

Advanced application of XPS to outline the first layer atomic structures of the bulk drug, polymers and the spray dried particles was implemented based on the hydrogen consumption approach. The chemical elemental surveys of the drug, polymer and active formulations are depicted in Fig. 5a. It shows that the drug contains about 54% of C while 17% O and about 34% N. The elemental ratios are in in good agreement with that of theoretically calculated values. In contrast, S100 predominantly contained 75% C while EZE contained O, C, Mg and Si as it is a co-processed polymer with crystalline substances and silica/Talc.

The peak fitting and data interpretation using the CasaXPS software determined the N (1s) binding energy (BE) at ~399.3 eV and ~402.0 eV corresponding to the two different N environments present in the INH structure (Fig. 5b). These two different N atoms may contribute to different types of protonation effects. The ratio between the two N environments may prove significantly important to determine and possibly outline the interactions between the drug and the anionic polymers.

The N (1s) BE values of ~402.0 eV in INH indicates the protonation effects of the NH^+ group. Interestingly, this has been shifted to ~402.7 eV in S100 system and ~402.9 eV for EZE (Fig. 5b). Apparently, these significant shifts in the BE values of N atoms are attributed to the interactions of the drug and the respective polymers. These also are due to the heavy protonation effect of N atoms in the spray dried particles resulting in the interaction via the amide group of the drug and the carboxyl group of the polymers [24-26]. The calculated low N coefficient values in the formulations revealed that the interactions between the drug and polymers are quite strong. It has been reported that the lower N coefficient value leads to a high number of protonated N atoms that take part in the interactions making it stronger [27-30].

3.6 In vitro dissolution studies

The main aim of this study was to evaluate the drug release behavior of the manufactured spray dried microencapsulated particles as INH is highly water soluble drug the release rate is very fast (>80% release in 1 h) [31]. The *in vitro* dissolution results are shown in Figures 6a and 6b. The drug/polymer ratio of 1:1 with three different polymers showed a different controlled release pattern for the first 2 h and then a burst release when the pH was increased to 6.8 (Fig. 6a). This could highly be attributed to the pH dependent dissolution of anionic S100 and EZE polymers. It has been reported that none of these polymers dissolved at pH below 6-6.5 [32]. In contrast, when ECN10 was used as the polymeric carrier, a relatively faster drug release was observed due to the pH independent dissolution of the polymer.

Interestingly, when the polymer content was increased in the formulations (drug: polymer ratio 1:3), the drug release seemed to reduce (Fig. 6b) due to the increased amount of the release retarding polymers which played a pivotal role to slow down the release of the highly soluble drug. Formulations containing S100, generally, showed a very slow release profile throughout the study for 12 h while for EZE, a faster release was observed when the pH was increased from 1.2 to 6.8 after 2 h. This could be due to the co-processed nature of the polymer and a bit lower pH dependency. Regardless of the formulation compositions, the release of the drug from all spray dried particles were controlled which proves the effective role of these polymers to develop controlled release formulations via spray dried encapsulation technique. ANOVA statistical test showed that for the same polymer the ratio of drug: polymer ratios have no significant effects on the drug release ($p>0.05$).

3.7 Release mechanism studies

The kinetic parameters derived from the various release kinetic models of the INH release are summarized in Table 3. The analysis of the correlation coefficient (R^2) in all models used indicated that the maximum R^2 was found in the First Order release kinetics model. Therefeore, analyses performed by DDSolver software revealed that the drug release mechanism followed a first order release kinetics (Table 3) for all of the formulations prepared.

4. Conclusions

A spray drying process was successfully implemented for the microencapsulation of isoniazid which proved a promising approach to develop controlled release dosage forms. The microscopic investigation showed that the obtained micro-particles were spherical in shape and a mean particle size less than 10 microns. The solid state analysis revealed the existence of the semi crystalline INH in the polymer matrices. The advanced surface analysis conducted by using EDS showed a homogeneous distribution of the drug in the polymeric spray dried particles while the first layer elemental analysis via XPS revealed a strong intermolecular interaction between the drug and the polymer used in all formulations. In addition, the manufactured particles showed a controlled (pH dependent) release of the soluble INH which proves that this emerging processing technology can successfully be implemented to develop modified release solid dosage forms.

Conflict of interest

The authors report no conflict of interest.

5. References

1. A. Paudel, Z.A. Worku, J. Meeus, S. Guns, G. Van den Mooter, Manufacturing of solid dispersions of poorly water soluble drugs by spray drying: formulation and process considerations, Int. J. Pharm. 453(1) (2013) 253–84.
2. B. Muñoz Ortega, M.A. Sallam, M.T. Marín Boscá, Methacrylate micro/nano particles prepared by spray drying: a preliminary in vitro/in vivo study, Drug Deliv. 23(7) (2016) 2439-2444.
3. J. Li, D. Patel, G. Wang, Use of Spray-Dried Dispersions in Early Pharmaceutical Development: Theoretical and Practical Challenges, AAPS J. (2016). doi:10.1208/s12248-016-0017-9.
4. D.T. Friesen, R. Shanker, M. Crew, D.T. Mithey, W.J. Curatolo, J.A.S. Nightingale, Hydroxypropyl methylcellulose acetate succiate-based spray-dried dispersions: an overview. Mol. Pharm. 5(6) (2008) 1003–19.
5. Wu , J. Li, Y. Wang, Evaluation of the microcentrifuge dissolution method as a tool for spray-dried dispersion, AAPS J. 18(2) (2016) 346–53.
6. M. Cano-Chauca, P.C. Stringheta, A.M. Ramos, J. Cal-Vidal, Effect of the carriers on the microstructure of mango powder obtained by spray drying and its functional characterization, Inn. Food Sci. Emerg. Technol. 5 (2005) 420-428.
7. S. Berg, M. Bretz, E.M. Hubbermann, K. Schwarz, Influence of different pectins on powder characteristics of microencapsulated anthocyanins and their impact on drug retention of shellac coated granulate, J Food Eng. 108 (2012) 158-165.
8. R.V. Tonon, C. Brabet, M.D. Hubinger, Anthocyanin stability and antioxidant activity of spray dried acai (Euterpe aleracea Mart.) juice produced with different carrier agents. Food Res Int. 43 (2010) 907-914.
9. Y. Wu, L. Zou, J. Mao, J. Huang, L. Shiwang, Stability and encapsulation efficiency of sulforaphane microencapsulated by spray drying, Carbohydr. Poly.102 (2014) 497-503.
10. C. Krzyszt, K. Sollohub, Spray Drying Technique. 1: Hardware and Process Parameters, J Pharm Sci. 99(2) (2010) 575-585.

11. D.M. Brahmankar and S.B. Jaiswal, Biopharmaceutics and Pharmacokinetics A Treatise, Vallabh Prakashan. (2007) 347-349.
12. S. Benita, Microencapsulation Methods and Industrial Applications, Taylor and Francis. (2006) 99-101.
13. R.A. Bayerinck, H. Deibele et al., Method for making homogenous spray dried solid amorphous drug dispersions utilizing modified spray-drying apparatus, US Patent (2004) 6: 763,607
14. G. Gjavaresi, M. Tschon et al., New polymers for Drug Delivery Systems in orthopedics in vivo biocompatibility evaluation, Biomed Pharm. 58 (2004) 411-417.
15. M. Kaur, T. Garg, R.K. Narang, A review of emerging trends in the treatment of tuberculosis Artif. Cells, Nanomed. Biotechnol. 44(2) (2016) 478-84.
16. A.K. Goyal, T. Garg T, G. Rath G, U.D. Gupta, P. Gupta, Development and Characterization of Nanoembedded Microparticles for Pulmonary Delivery of Antitubercular Drugs against Experimental Tuberculosis, Mol. Pharm. 12(11) (2015) 3839-50.
17. M. Poggi, R. Barroso, A. J. Costa-Filho, H. B. de Barros, F. Pavan, C. Q. Leite, D. Gambino, M. H. Torre, New Isoniazid Complexes, Promising Agents Against Mycobacterium tuberculosis, J. Mex. Chem. Soc. 57(3) (2013) 198-204.
18. Y. Zhang, M. Huo, J. Zhou, A. Zou, W. Li, C. Yao, S. Xie, DDSolver: An Add-In Program for Modeling and Comparison of Drug Dissolution Profiles, AAPS J. 12 (2010) 263-271.
19. K.D. Tripathi, Essentials of Medical Pharmacology, Jaypee (2009) 739-741.
20. G. Gjavaresi, M. Tschon et al., New polymers for Drug Delivery Systems in orthopedics in vivo biocompatibility evaluation. Biomed. Pharm. 58 (2004) 411-417.
21. M. Maniruzzaman, S. Farias, I.J. Slipper, J. S. Boateng, B.Z. Chowdhry, A. Nair, D. Douroumis, Development and optimization of ketoconazole oral strips by means of

continuous hot-melt extrusion processing, J. Pharm. Pharmacol. 2016; in press. doi: 10.1111/jphp.12569.

22. R.A. Carlton, Scanning Electron Microscopy and Energy-Dispersive X-Ray Spectrometry. Pharmaceutical microscopy. Springer, USA. (2011) 85-130.
23. C. Bruce, K.A. Fegely, A.R. Rajabi-Siahboomi, J.W. McGinity, Crystal growth formation in melt extrudates, Int. J Pharm. 341(1-2) (2007) 162-72.
24. G. Beamson, D. Briggs, High resolution XPS of organic polymers: The Scienta ESCA 300 Database, J Chem. Educ. (1993) 70 PA25.
25. N. Vandencasteele, F. Reniers, Plasma-modified polymer surfaces: Characterization using XPS, J Elec. Spe.c Rel. Phenom. 178–179 (2010) 394–408.
26. P. Ghods, O.B. Isgor, J.R. Brown, F. Benseba, D. Kingston, XPS depth profiling study on the passive oxide film of carbon steel in saturated calcium hydroxide solution and the effect of chloride on the film properties, App. Sur. Sci. 257 (2011) 4669–4677.
27. M. Maniruzzaman, D.J. Morgan, A.P. Mendham, J. Pang, M.J. Snowden, D. Dououmis, Drug-polymer intermolecular interactions in hot-melt extruded solid dispersions, Int. J Pharm. 443(1-2) (2013) 199-208.
28. M. Maniruzzaman, J. Pang, D.J. Morgan, D. Douroumis, Molecular modelling as a predictive tool for the development of solid dispersions, Mol. Pharm. 12(4) (2015) 1040-9.
29. M. Maniruzzaman, M.S.A. Bradley, M.J. Snowden, D. Douroumis, Studies of intermolecular interactions in solid dispersions using advanced surface chemical analysis, RSC Adv. 5 (2015) 74212-74219.
30. D. Palmer, M. Levina, D. Douroumis, M. Maniruzzaman, D.J. Morgan, T.P. Farrell, A.R. Rajabi-Siahboomi, A. Nokhodchi, Mechanism of synergistic interactions

and its influence on drug release from extended release matrices manufactured using binary mixtures of polyethylene oxide and sodium carboxymethylcellulose, Colloids Surf. B Bio. 104 (2013) 174-80.

31. US Pharmacopia, http://www.pharmacopeia.cn/v29240/usp29nf24s0_m43010.html. Last accessed on June 2016.
32. M.Z. Khan, H.P. Stedul, N. Kurjaković, A pH-dependent colon-targeted oral drug delivery system using methacrylic acid copolymers. II. Manipulation of drug release using Eudragit L100 and Eudragit S100 combinations, Drug Dev. Ind. Pharm. 26(5) (2000) 549-54.

TABLES

Table 1. Parameters for spray drying of INH loaded microparticles with B-290, drug loading (DL) and encapsulation efficiency (EE).

	Formulations	**Inlet Temp (^{0}C)**	**Aspirator**	**Feed flow (%)**	**Pressure (mbar)**	**Yield (%)**	**DL* (%)**	**EE* (%)**
F1	INH/S100 (1:1)	100	90	13	25	67	40.6	81.2
F2	INH/S100 (1:3)	100	90	13	25	64	22.8	91.2
F3	INH/EZE (1:1)	100	90	15	20	63	40.5	81.0
F4	INH/EZE (1:3)	100	90	15	20	64	23.6	94.4
F5	INH/EC10 (1:1)	100	90	13	35	72	45.1	90.2
F6	INH/EC10 (1:3)	100	90	13	35	82	22.8	91.2

DL=Drug loading; EE= Encapsulation efficiency

Table 2: Particle morphology and characteristics of various spray dried controlled release particles.

	F1	**F2**	**F3**	**F4**	**F5**	**F6**
d_{10} (μm)	1.2±0.02	1.2±0.01	1.3±0.00	1.3±0.00	1.3±0.04	1.3±0.00
d_{50} (μm)	5.7±0.01	5.7±0.01	5.9±0.01	5.9±0.00	6.0±0.01	6.0 ±0.00
d_{90} (μm)	8.9±0.04	9.1±0.02	9.4±0.01	8.3±0.01	8.4±0.16	8.2±0.01
<1 (μm)	8.2±0.71	9.0±0.20	7.7±0.20	9.4±0.01	8.0±0.8	7.8±0.02
SSA (m^2/g)	68.15±0.50	75.80±0.10	96.30±0.20	106.90±0.07	91.50±0.01	95.40±0.05
Bulk density (g/cm^3)	0.15±0.01	0.15±0.01	0.16±0.01	0.14±0.00	0.13±0.01	0.15±0.00
Tapped density (g/cm^3)	0.23±0.01	0.25±0.05	0.26±0.02	0.23±0.03	0.22±0.01	0.28±0.02
LoD	2.21±0.15	1.80±0.20	2.15±0.20	1.25±0.15	2.13±0.15	2.26±0.10

Table 3: Summary of release mechanism of INH from various formulations

Model	**Parameter**	**F1**	**F2**	**F3**	**F4**	**F5**	**F6**	**INH**
Zero-order	K_0	8.86	6.15	10.53	10.38	10.93	7.72	12.5
	r^2	0.81	0.78	0.764	0.807	0.730	0.630	0.546
First-order	K_1	0.24	0.12	0.40	0.32	0.61	0.30	1.72
	r^2	0.937	0.874	0.958	0.943	0.982	0.847	0.999
Higuchi	K_h	26.69	19.62	32.74	31.28	35.32	25.70	42.55
	r^2	0.902	0.935	0.893	0.899	0.905	0.835	0.778
Korsmeyer-Peppas	K_{kp}	21.43	28.24	32.51	25.01	51.37	45.74	76.97
	n	0.62	0.29	0.51	0.62	0.29	0.15	0.33
Hixson-Crowell	K_{Hc}	0.07	0.033	0.107	0.094	0.120	0.088	0.13
	r^2	0.940	0.843	0.961	0.950	0.952	0.834	0.821

Figures caption list:

Figure 1 Chemical structures of the drug and the polymers used.

Figure 2a SEM images of the encapsulated spray dried INH loaded micro-particles.

Figure 2b EDS mapping of bulk INH and the INH/S100 formulations.

Figure 3 XRPD diffractograms of bulk INH and the spray dried formulations.

Figure 4a DSC thermal transitions of bulk drug and the polymers.

Figure 4b DSC traces of the spray dried INH loaded micropartciles.

Figure 5a Chemical elemental surveys conducted via XPS using CasaXPS software.

Figure 5b Peak fitting of N (1s) binding energy of the drug and the spray dried particles with S100 and EZE polymers.

Figure 6 *In vitro* dissolution studies of INH pure and the spray dried micropartciles at (a) drug/polymer 1:1 ratio and (b) drug/polymer 1:3 ratio (n=3).

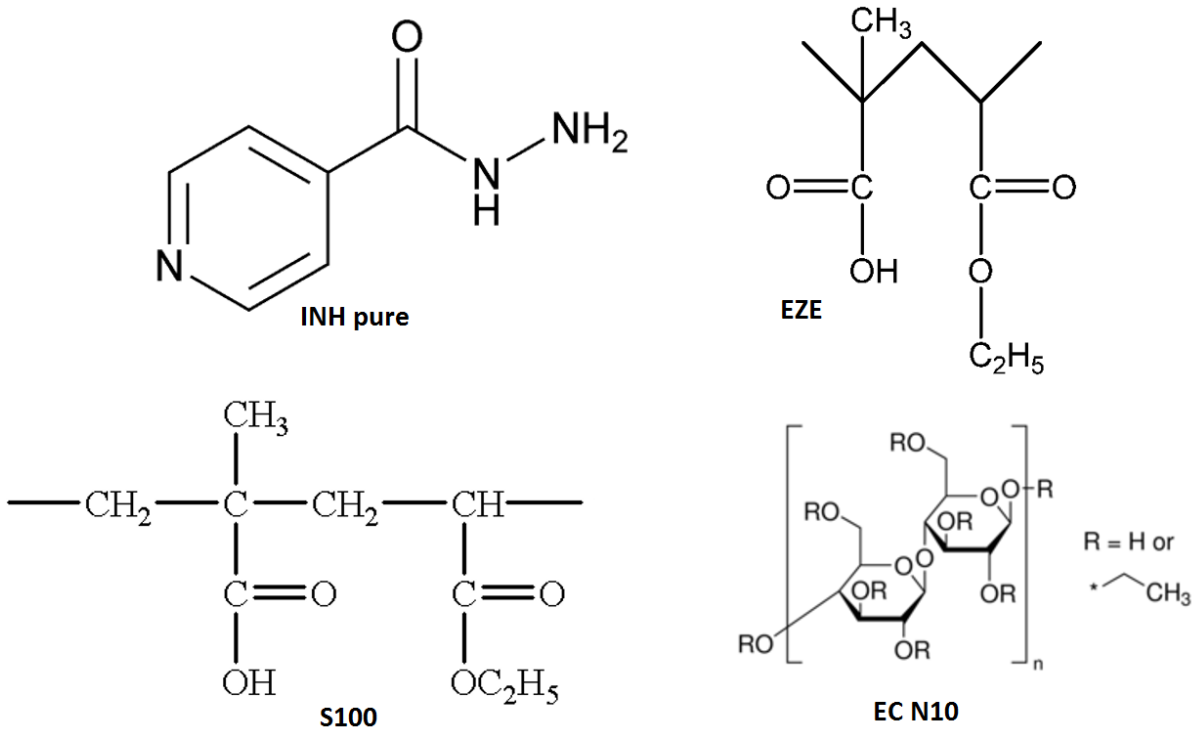

Fig. 1

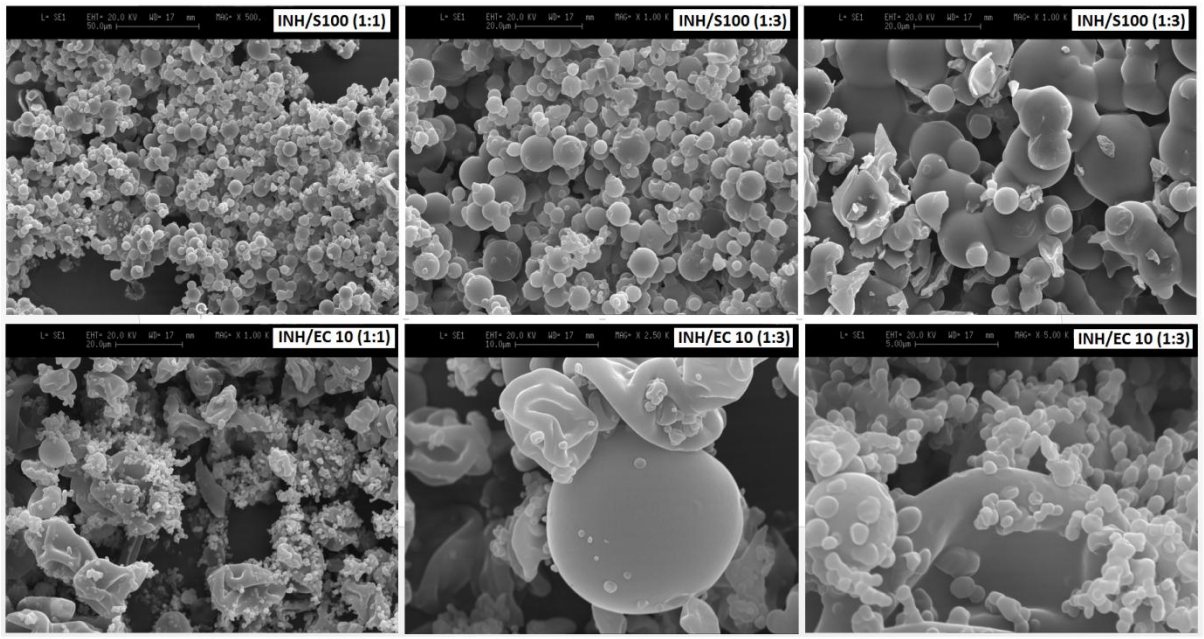

Fig. 2a

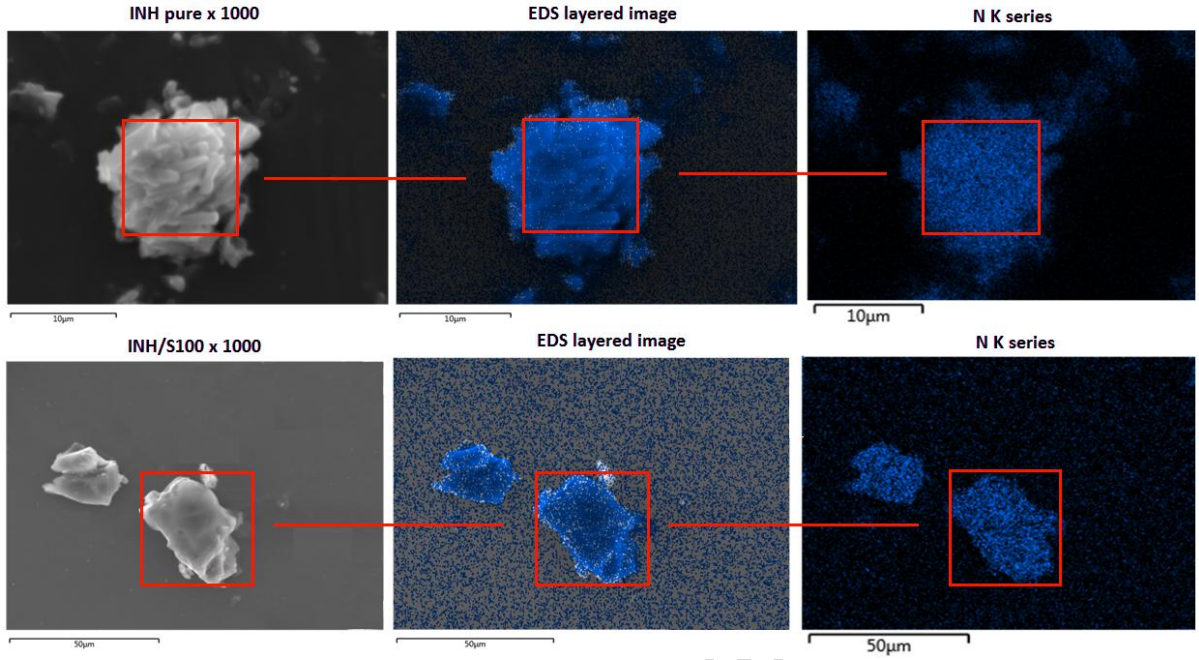

Fig. 2b

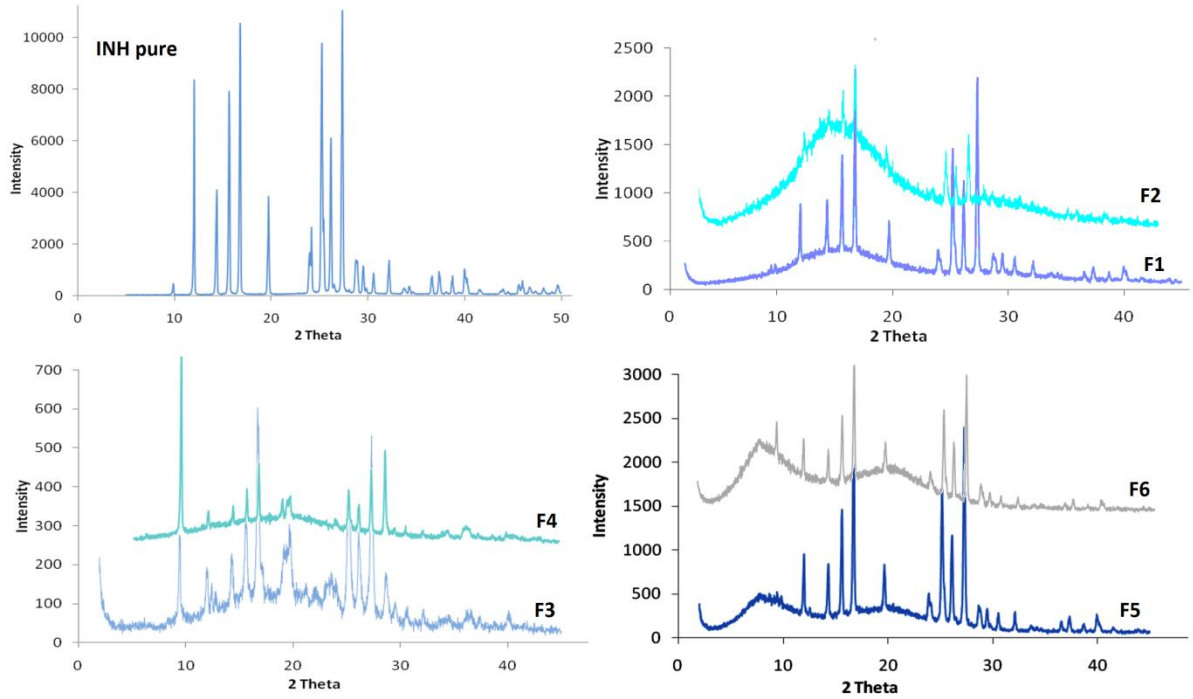

Fig. 3

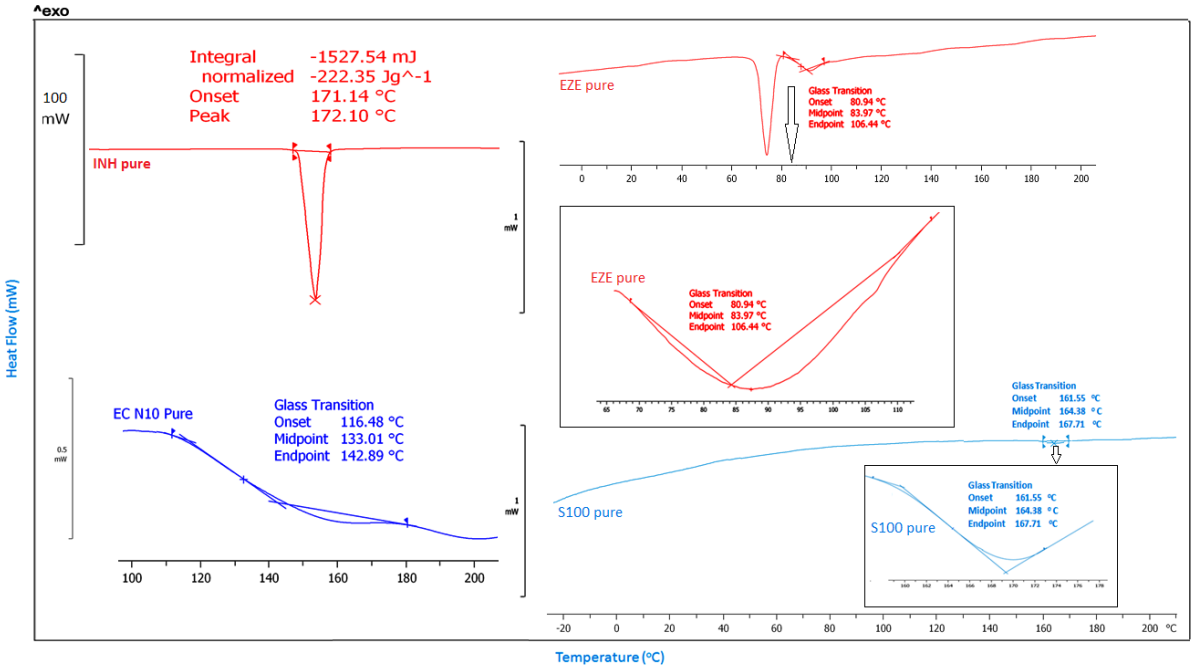

Fig. 4a

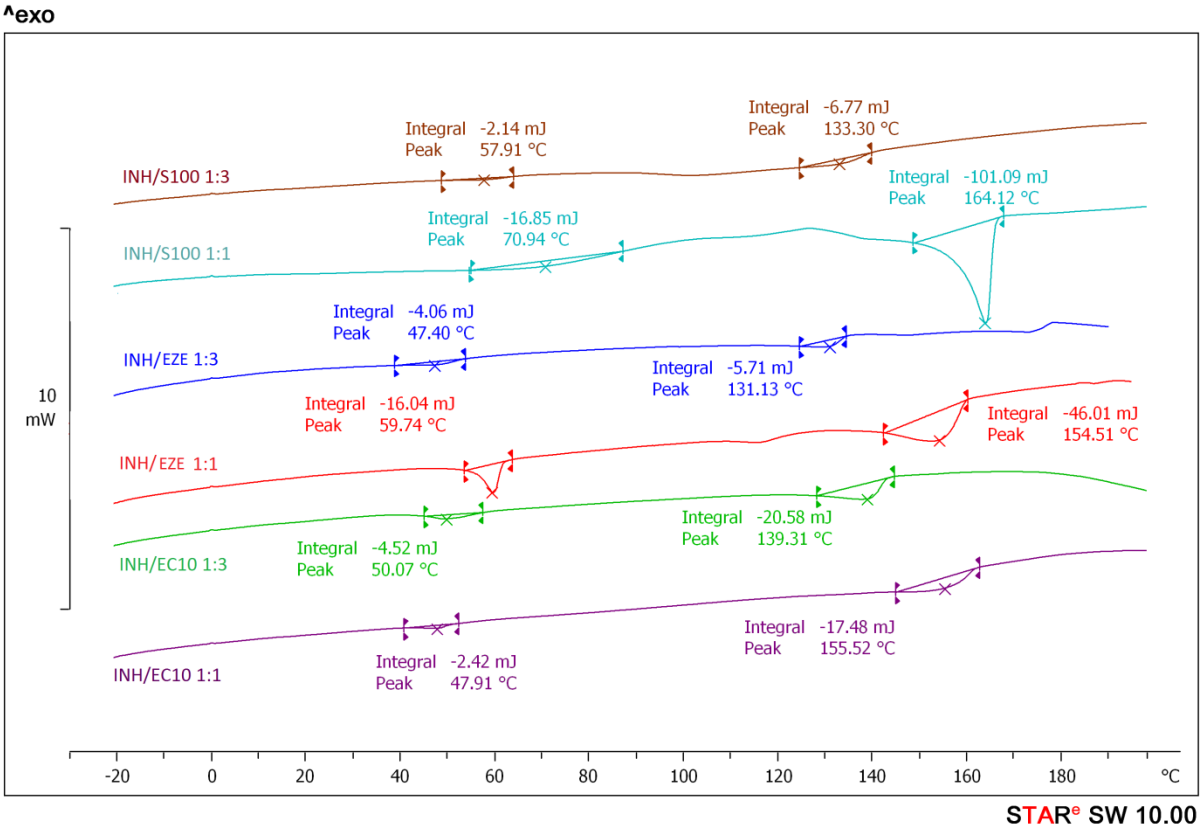

Fig. 4b

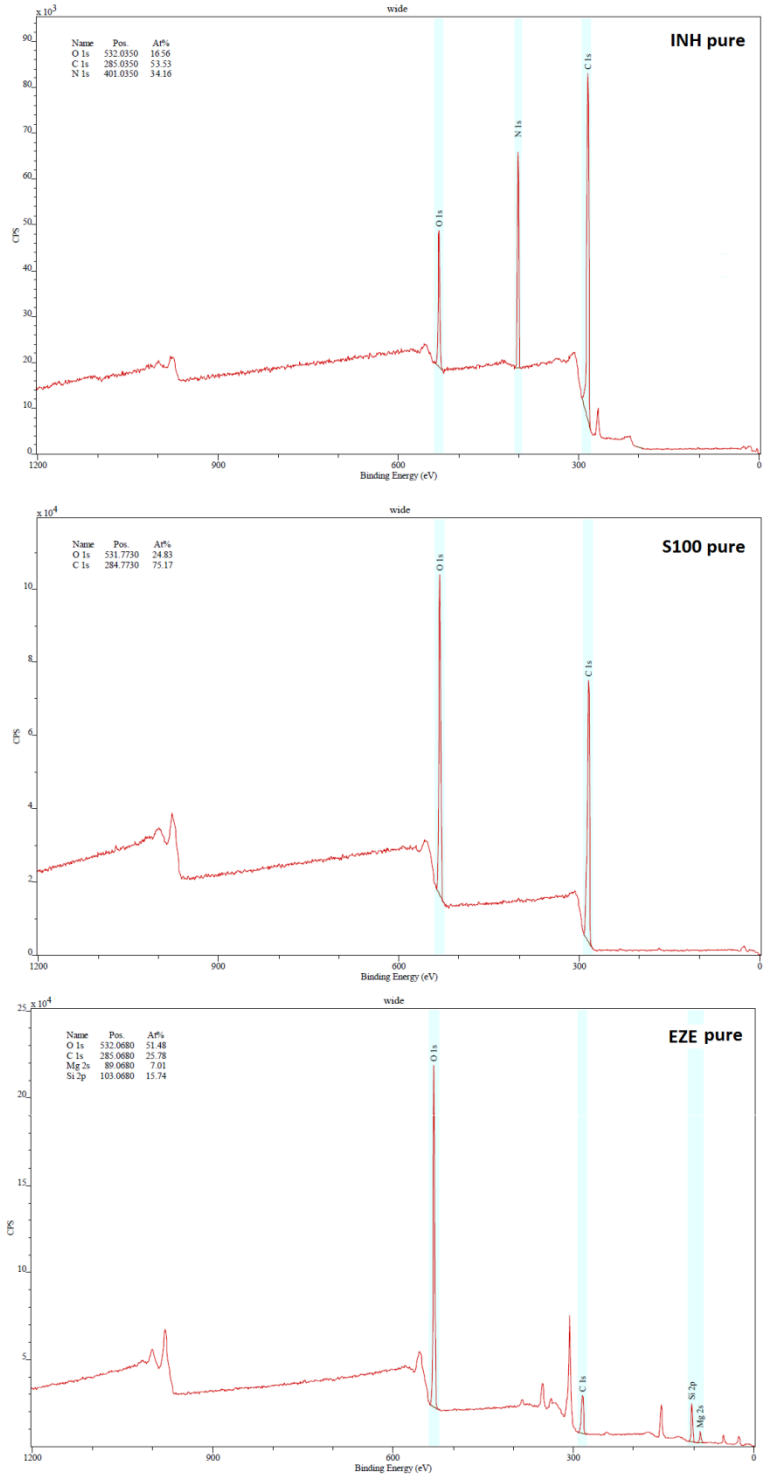

Fig. 5a

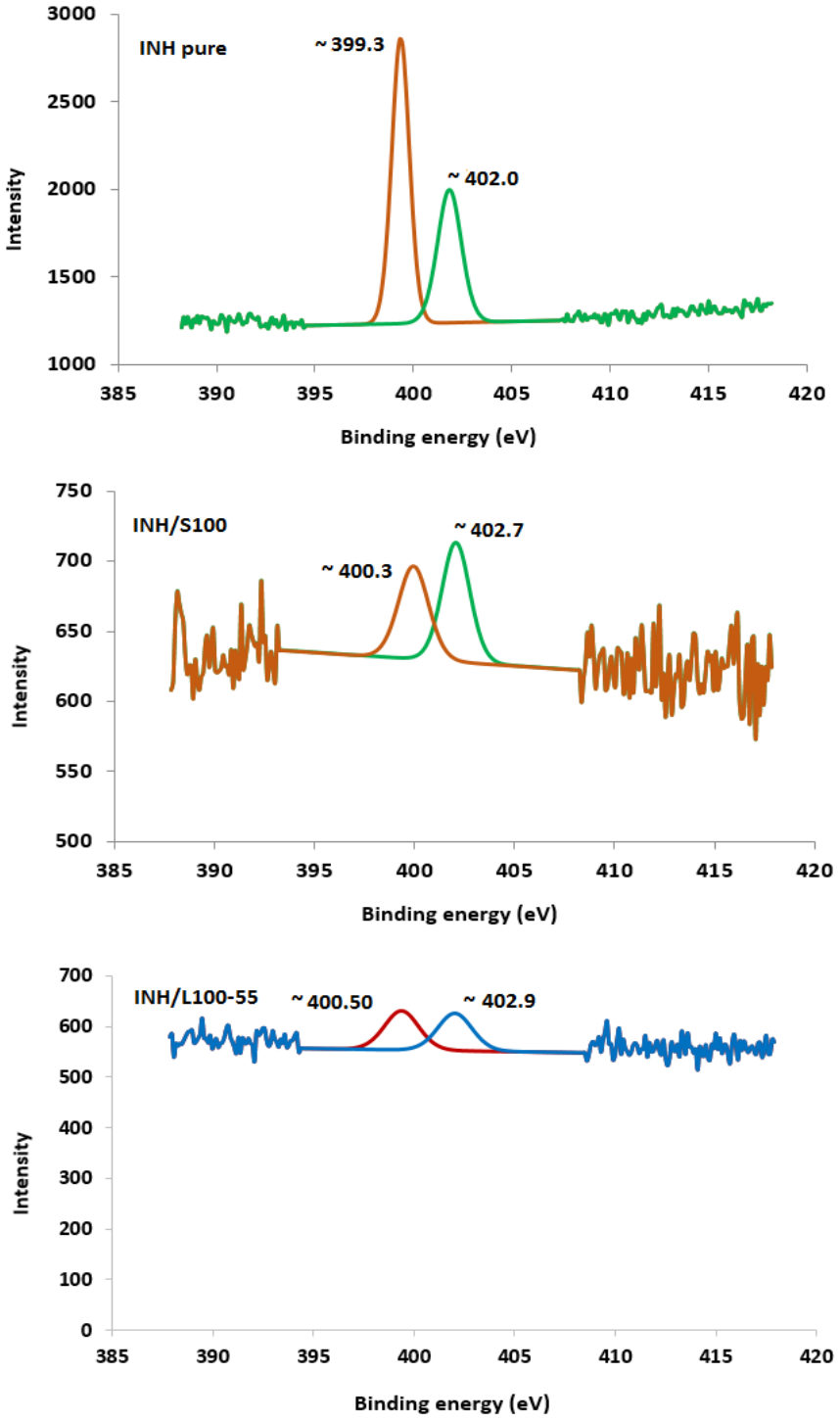

Fig. 5b

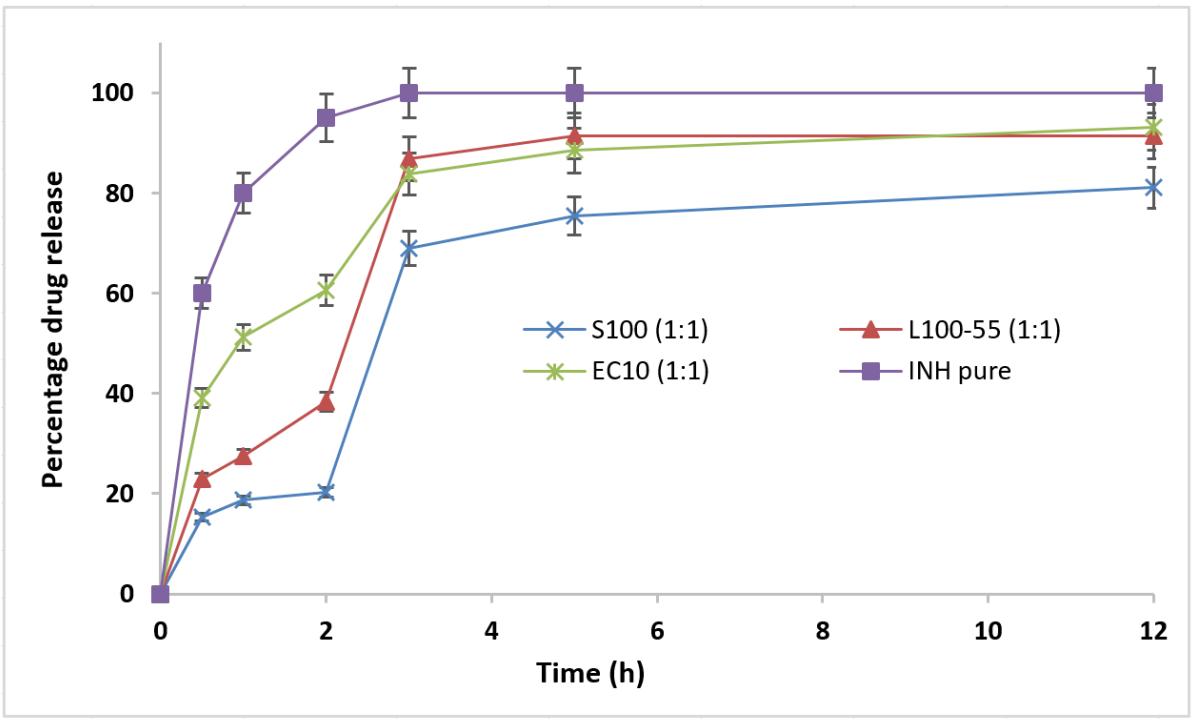

(a)

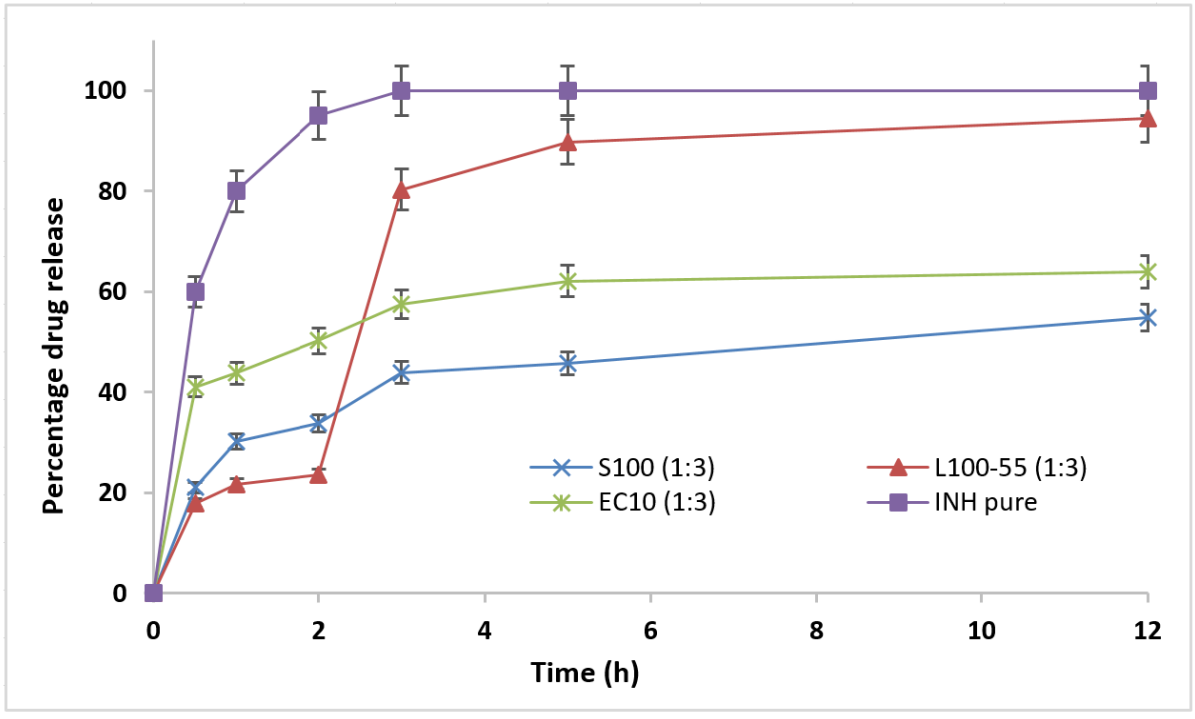

(b)

Fig. 6

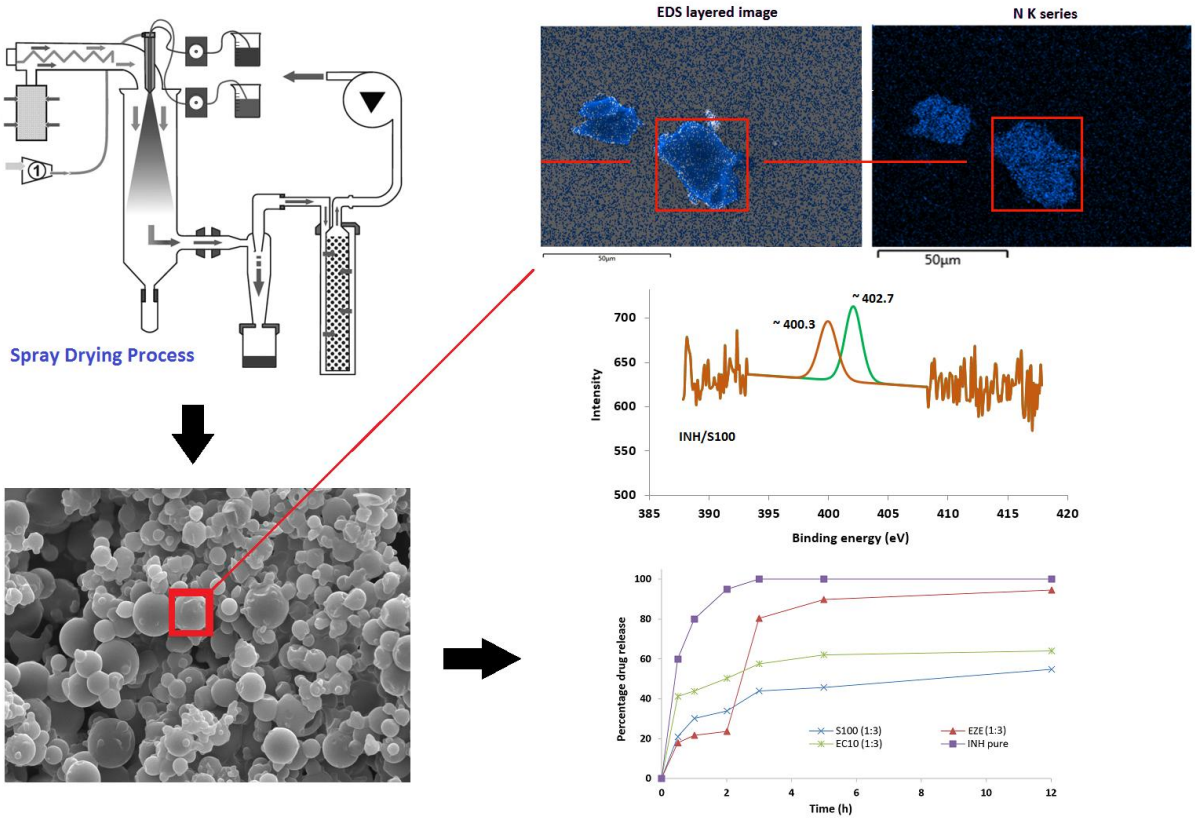

Graphical Abstract

Highlights:

- The surface chemistry plays a pivotal role in micro-encapsulations
- Suitable polymers are important to manufacture controlled release micro-particles
- EDX analyses the drug distribution on the particle surface
- XPS outlines a possible interaction pattern between the drug and carriers
- Optimised process and formulations control release of highly soluble drug